

1 **Title**

2 Genomic insights into adaptations of TMA-utilizing methanogens to diverse habitats
3 including the human gut

4 **Running title**

5 Insights into *Methanomassiliicoccales* in the human gut

6

7 **Authors**

8 Jacobo de la Cuesta-Zuluaga¹, Timothy D. Spector², Nicholas D. Youngblut¹, Ruth
9 E. Ley^{1#}

10

11 ¹Department of Microbiome Science, Max Planck Institute for Developmental
12 Biology, 72076 Tübingen, Germany.

13

14 ²Department of Twin Research and Genetic Epidemiology, King's College London,
15 London SE1 7EH, UK

16

17 # correspondence: rley@tuebingen.mpg.de.

18 **Abstract**

19 Archaea of the order *Methanomassiliicoccales* use methylated-amines such
20 as trimethylamine as a substrate for methane production. They form two large
21 phylogenetic clades and reside in diverse environments, from soil to the human gut.
22 Two genera, one from each clade, inhabit the human gut: *Methanomassiliicoccus*,
23 which has one cultured representative, and “*candidatus* Methanomethylophilus”,
24 which has none. Questions remain regarding their distribution across different
25 biomes and human populations, their association with other taxa in the human gut,
26 and whether host genetics correlate with their abundance. To gain insight into the
27 *Methanomassiliicoccales*, and the human-associated members in particular, we
28 performed a genomic comparison of 72 *Methanomassiliicoccales* genomes and
29 assessed their presence in metagenomes derived from the human gut (n=4472
30 representing 25 populations), nonhuman animal gut (n=145) and nonhost
31 environments (n=160). Our analyses showed that all taxa are generalists: they were
32 detected in animal gut and environmental samples. We confirmed two large clades,
33 one enriched in the gut, the other enriched in the environment, with notable
34 exceptions. Genomic adaptations to the gut include genome reduction, a set of
35 adhesion factors distinct from that of environmental taxa, and genes involved in the
36 shikimate pathway and bile resistance. Genomic adaptations differed by clade, not
37 habitat preference, indicating convergent evolution between the clades. In the
38 human gut, the relative abundance of *Methanomassiliicoccales* correlated with
39 trimethylamine-producing bacteria and was unrelated to host genotype. Our results
40 shed light on the microbial ecology of this group may help guide
41 *Methanomassiliicoccales*-based strategies for trimethylamine mitigation in
42 cardiovascular disease.

43 **Importance**

44 *Methanomassiliicoccales* are a lesser known component of the human gut
45 microbiota. This archaeal order is composed of methane producers that use
46 methylated amines, such as trimethylamine, in methane production. This group has
47 only one cultured representative; how they adapted to inhabit the mammalian gut
48 and how they interact with other microbes is largely unknown. Using bioinformatics
49 methods applied to DNA from a wide range of samples, we profiled the relative
50 abundances of these archaea in environmental and host-associated microbial
51 communities. We observed two groups of *Methanomassiliicoccales*, one largely
52 host-associated and one largely found in environmental samples, with some
53 exceptions. When host-associated, these archaea have a distinct set of genes
54 related to adhesion and possess genes related to bile resistance. We did not detect
55 *Methanomassiliicoccales* in all human populations tested but when present, they are
56 correlated with *Bacteria* known to produce trimethylamine. Since trimethylamine is
57 linked to cardiovascular disease risk, these intriguing Archaea may also be involved.

58 Introduction

59 *Archaea* generally make up a tenth or less of the biomass of the human gut
60 microbiota; however, they are widely prevalent and occupy a unique metabolic niche,
61 utilizing by-products of bacterial metabolism as substrate for methanogenesis (1).
62 The most widespread methanogens in the human gut are members of the order
63 *Methanobacteriales*. These include *Methanobrevibacter smithii*, which uses CO₂,
64 formate and H₂ as substrates for methane production (2), and *Methanosphaera*
65 *stadtmanae*, which consumes methanol and H₂ (3). Through the process of methane
66 formation, *Archaea* decrease partial pressures of H₂, thereby potentially increasing
67 the energetic efficiency of primary fermenters and the production of short-chain fatty
68 acids (4). Members of *Methanobacteriales* are the dominant species of the human
69 gut archaeome (1, 5).

70 A second archaeal lineage, the order *Methanomassiliicoccales*, is also found
71 within the human gut microbiota, yet its members are less well characterized than
72 those of *Methanobacteriales*. Members of the order *Methanomassiliicoccales*,
73 including human-derived *Methanomassiliicoccus luminyensis*, “*candidatus*
74 *Methanomassiliicoccus intestinalis*” and “*candidatus* *Methanomethylophilus alvus*”,
75 perform H₂-dependent methylotrophic methanogenesis as sole energy source (6–8).
76 Their genomes encode several methyltransferases and associated proteins used to
77 reduce methylamines and methanol to methane. Studies based on 16S rRNA and
78 *mcrA* gene diversity analysis indicate that the order *Methanomassiliicoccales* is
79 made up of two large clades, which mostly group species that have either a free
80 living (FL) or host associated (HA) lifestyle (9, 10). Based on analyses of the
81 genomes from three human-derived species from both clades, Borrel *et al.* (11)
82 suggested each clade colonized the mammalian gut independently. Members of the

83 HA clade, including the human-associated “*ca. M. alvus*”, might be expected to show
84 adaptations similar to other methanogens from the gut microbiota (12, 13). How
85 members of the FL clade, including the human-associated *M. luminyensis* and “*ca.*
86 *M. intestinalis*”, have converged on the gut niche remains to be explored.

87 A better understanding of the ecology of *Methanomassiliicoccales* may be of
88 interest to human health, as they can utilize mono-, di-, and trimethylamine (TMA) as
89 substrate for methanogenesis in the gut (14). TMA, a by-product of the bacterial
90 metabolism of carnitine, choline, and other and choline-containing compounds, is
91 absorbed by the host and transformed in the liver into trimethylamine N-oxide
92 (TMAO) (15). In turn, circulating TMAO inhibits cholesterol transport and promotes
93 its accumulation in macrophages, inducing the formation of atherosclerotic plaques
94 (16). Decreasing TMA levels in the gut, and reducing circulating TMAO levels, has
95 been proposed as a therapeutic strategy for cardiovascular disease (17). One way to
96 use the gut microbiome to this end would be to boost levels of
97 *Methanomassiliicoccales* (18). To accomplish this goal requires a deeper
98 understanding of its ecology.

99 Here, we conducted a comparative analysis of 71 *Methanomassiliicoccales*
100 genomes, together with an additional metagenome-assembled genome (MAG)
101 corresponding to a strain of “*ca. M. alvus*”, which we retrieved by metagenome
102 assembly of gut samples from subjects of the TwinsUK cohort (19). We used 305
103 publically available metagenomes to assess the prevalence of taxa across various
104 habitat types. While the two large clades grouping host-associated (HA) and free-
105 living (FL) taxa, are generally enriched in host-associated and environmental
106 metagenomes, a few exceptions stand out. Our results showed that the repertoire of
107 adhesion proteins encoded by the genomes of taxa from each clade differed. Genes

108 involved in bile resistance and the shikimate pathway are likely involved in the
109 adaptation to the gut environment of members of the HA clade, but not for the FL
110 clade. Thus, gut-adapted members converged on life in the gut using different
111 genomic adaptations. *Methanomassiliicoccales* genera present in the human gut
112 positively correlate with TMA-producing bacteria.

113

114 **Materials and Methods**

115 ***Genome annotation and phylogenomic tree reconstruction***

116 We downloaded 78 available genomes belonging to the order
117 *Methanomassiliicoccales* from the NCBI assembly database
118 (<https://www.ncbi.nlm.nih.gov/assembly>) as available in June 2018, and used
119 CheckM to assess their quality. For subsequent analyses, we included 71
120 substantially complete genomes (completeness $\geq 70\%$) with low contamination
121 (contamination $< 5\%$) (20), plus an additional high-quality metagenome-assembled
122 genome (MAG) corresponding to “*candidatus* Methanomethylophilus alvus” (see
123 *supplementary methods* and table S1). Gene calling, proteome prediction and
124 annotation was performed on each genome using Prokka 1.12 (21). Details of each
125 genome, including the original source of isolation, can be found in (table S1).

126 Using PhyloPhlAn 0.26 (22), we constructed a maximum-likelihood
127 phylogenomic tree using a concatenated alignment of multiple universally distributed
128 single copy marker genes of 72 publicly available genomes from the order
129 *Methanomassiliicoccales*. Of these, one was retrieved from pure culture, 6 were
130 obtained from enrichment cultures and 64 were MAGs. We included an additional
131 MAG retrieved from human gut metagenomes corresponding to “*ca. M. alvus*”
132 (*supplementary results*). Briefly, universal markers were obtained from the translated

133 amino acid sequences of the included genomes, aligned using mafft 7.3 (23) and
134 concatenated into a single sequence. We then used the concatenated alignment to
135 reconstruct an maximum-likelihood phylogenetic tree using RAxML 8.1 (24); branch
136 support was estimated by 1000 bootstrap iterations and the tree was rooted by
137 including members of the order *Thermoplasmatales* as outgroup, namely
138 *Thermoplasma acidophilum* DSM 1728 (GenBank assembly accession:
139 GCA_000195915.1), *Picrophilus oshimae* DSM 9789 (GCA_900176435.1),
140 *Ferroplasma acidarmanus fer1* (GCA_000152265.2), *Acidiplasma aeolicum*
141 (GCA_001402945.1) and *Cuniculiplasma divulgatum* (GCA_900090055.1). We used
142 iTOL (25) to visualize the tree.

143

144 ***Abundance of Methanomassiliicoccales in environmental and animal*** 145 ***gastrointestinal metagenomes***

146 We retrieved 305 metagenome samples of gastrointestinal and environmental
147 origin (26) sequenced using the Illumina HiSeq platform (table S2). Sequences were
148 then downloaded from the Sequence Read Archive (SRA) and quality-controlled
149 (see *supplementary methods*). To avoid the issue of multiple mapping, we
150 dereplicated the 72 genomes at a species-level threshold (95 % ANI) using dRep,
151 resulting in 29 representative genomes. Next, we quantified the abundance of
152 dereplicated *Methanomassiliicoccales* genomes in these samples using KrakenUniq
153 v.0.5.8 (27). Statistical analyses were performed using R v.3.5.1 (28). We estimated
154 the enrichment of each representative *Methanomassiliicoccales* on host or
155 environmental metagenomes using DESeq2 (29) on sequence counts and
156 classifying metagenome samples as either host-derived or environmental. We
157 applied hierarchical clustering using Ward's method on the log-fold-change of

158 environmental vs gastrointestinal enrichment of each taxon and calculated the
159 cophenetic correlation with the phylogenomic tree using the ape package of R (30).

160

161 ***Comparative genomics***

162 The predicted proteome of each included genome was used to to assign
163 orthology clusters using panX 1.6.0 (31). We used InterProScan (32) and eggNOG
164 mapper 1.0.3 (33) with DIAMOND 0.8.36 (34) against the optimized archaeal
165 database to improve the annotation of gene clusters. Phylogenetic signal of genome
166 characteristics and gene cluster presence was tested using the phylosignal package
167 of R with the local indicator of phylogenetic association (LIPA) (35).

168 The R package micropan (36) was used to create a principal component
169 analysis (PCA) of gene cluster presence. We compared the gene cluster content
170 between clades to determine gene clusters enriched on clades FL or HA using
171 phylogenetic ANOVA using the R package phytools (37). To reduce the number of
172 comparisons we first removed low frequency gene clusters by filtering those with
173 near zero variance. The above analysis was repeated by comparing gene cluster
174 content between taxa significantly enriched on gut or environmental samples, prior
175 removal of taxa not significantly enriched in either biome class. We adjusted P
176 values with the Benjamini-Hochberg method.

177 We assessed the presence of eukaryote-like proteins (ELPs) (38) by
178 combining the counts of gene clusters classified by InterProScan as any of the
179 following: Sel1 containing proteins (Sel1), Listeria-Bacteroides repeat containing
180 proteins (List-Bact), tetratricopeptide repeats (TPRs), Ankyrin repeats (ANKs),
181 Leucine-rich repeats (LRRs), Fibronectin type III (fn3) domains, Laminin G domain,
182 Bacterial Ig-like domains, YadA-like domain (Yersinia adhesin A), TadE-like domain

183 or Invasion protein B (IalB). Likewise, we characterized the presence of parallel beta-
184 helix repeat-containing proteins, also known as adhesin-like proteins (ALPs).

185

186 ***Characterization of Methanomassiliicoccales distribution across human*** 187 ***populations***

188 We obtained sample metadata from publicly available studies using the
189 curatedMetagenomicData v.1.17.0 package of Bioconductor (39). Samples were
190 selected according to the following criteria: i) shotgun gut metagenomes sequenced
191 using the Illumina HiSeq platform with a median read length > 95 bp; ii) with
192 available SRA accession; iii) labeled as adults or seniors, or with a reported age ≥ 18
193 years; iv) without report of antibiotic consumption (i.e. no or NA); v) without report of
194 pregnancy (i.e. no or NA); vi) non-lactating women (i.e. no or NA); vii) without report
195 of gangrene, pneumonia, cellulitis, adenoma, colorectal cancer, arthritis, Behcet's
196 disease, cirrhosis or inflammatory bowel disease. Only forward reads were
197 downloaded and processed. A total of 4472 samples from 34 independent studies
198 were downloaded from the SRA between December 2019 and February 2020 (table
199 S3) and quality controlled as described in *supplementary methods*.

200 Reads were classified using Kraken v.2.0 (40) and a Bayesian re-estimation
201 of the species-level abundance of each sample was then performed using Bracken
202 v.2.2 (41). We utilized custom databases created using the Struo pipeline (42) based
203 on GTDB release 86 (available at <http://ftp.tue.mpg.de/ebio/projects/struo/>). Taxa
204 with <100 reads in a given sample were considered as absent. We obtained
205 complete taxonomic annotations from NCBI taxIDs with TaxonKit 0.2.4
206 (<https://bioinf.shenwei.me/taxonkit/>). To determine the cooccurrence patterns of the
207 detected *Methanomassiliicoccales* in the human gut we used the cooccur package of

208 R (43); to determine their coabundance patterns, we calculated the proportionality of
209 taxa abundance (*rho*) with the *propr* package (44). The *lme4* and *lmerTest* R
210 packages (45) were used to fit linear mixed effects models to test differences of
211 *Methanomassiliicoccales* genera log-transformed abundance by westernization
212 status, age and gender with F-tests and P-values determined via the Satterthwaite's
213 method (ANOVA Type II sum of squares). Similarly, we employed binomial linear
214 mixed models to test differences of *Methanomassiliicoccales* genera prevalence.

215 We assessed the heritability of *Methanomassiliicoccales* taxa by comparing
216 relative abundances within 153 monozygotic (MZ) and 200 dizygotic (DZ) twin pairs
217 using the taxonomic profiles of 706 gut metagenome samples from the United
218 Kingdom Adult Twin Registry (TwinsUK) (19, 46, 47) with a sequencing depth >5
219 million reads/sample. We aggregated abundances at the genus level and removed
220 genera with a prevalence <5 %. Absolute read counts were transformed using the
221 Yeo-Johnson transformation and adjusted by BMI, sex and sequencing depth (19,
222 46). For each genus, we calculated the intraclass correlation coefficient (ICC) in MZ
223 and DZ twins with the *irr* package of R, and adjusted P-values for multiple
224 comparisons using the Benjamini-Hochberg method. As control we compared the
225 mean ICC across all taxa between MZ and DZ twins using the Mann-Whitney test,
226 and by assessing the ICC of specific taxa known previously reported as heritable in
227 the same population (*Methanobrevibacter*, *Faecalibacterium*, *Christensenella* and
228 *Bifidobacterium*) (46, 48). We carried a sensitivity analysis by repeating these
229 analyses on a subset of 394 samples (80 MZ and 117 DZ twin pairs) with a
230 sequencing depth of >12 million reads/sample.

231

232 **Data and code availability**

233 The metagenomic sequence data generated during this study have been
234 deposited in the European Nucleotide Archive with accession ID PRJEB40256. The
235 jupyter notebooks with analysis code are available at
236 <https://github.com/leylabmpi/Methanomassilii>. The "*candidatus*
237 *Methanomethylophilus alvus*" MAG here generated can be found at
238 <http://ftp.tue.mpg.de/ebio/projects/Mmassilii>

239

240 **Results**

241 ***Genome-based phylogeny confirms two large Methanomassilioccales clades***

242 Based on whole-genome phylogenetic analysis, the order
243 *Methanomassilioccales* forms two clades with robust support (figure 1). This
244 phylogeny is in agreement with previously reported phylogenies based on 16S rRNA
245 and *mcrA* genes (9, 49, 50). A third distal clade was formed by two closely related
246 MAGs generated in a recent massive metagenome assembly effort (51), which we
247 labeled external (EX; figure 1). We use the terminology of Borrel *et al.*, (52): the
248 clade including *Methanomassiliococcus* is labeled free-living (FL), and the clade
249 containing "*candidatus Methanomethylophilus*" host-associated (HA).

250 As observed previously (9), the reported source of the genomes was not
251 always consistent with the clade in which it was grouped. For instance, while publicly
252 available genomes originally retrieved from human, baboon, elephant and cow
253 gastrointestinal tracts were related to "*candidatus Methanomethylophilus*" (HA), this
254 clade also contained MAGs derived from digester and reactors (figure 1) reportedly
255 not treating animal waste (table S1). Moreover, MAGs retrieved from pit mud of
256 solid-state fermentation reactors used for the production of Chinese liquor were

257 present in both the HA and FL clades (table S1). Similarly, “*ca. M. intestinalis*”
258 Issoire-Mx1, *M. luminyensis* B10, and Methanomassiliicoccales archaeon RumEn
259 M1, all retrieved from mammal hosts, grouped in the FL clade.

260

261 ***Abundance of Methanomassiliicoccales clades differs in gastrointestinal and***
262 ***environmental samples***

263 We assessed the abundance of species-level representative
264 *Methanomassiliicoccales* taxa in publicly available metagenomes that included 145
265 samples from gastrointestinal tracts of non-human animals, such as cats, pigs, elks,
266 cows, sheep, mice, white-throated woodrats, trouts, chickens and geese, and 160
267 environmental samples from sediment, ice, and diverse water and soil sources (table
268 S2).

269 Taxa from all three clades were detected in a wide range of metagenomes
270 from environmental and gut origin. We observed differences in environmental
271 preference by clade. Abundance of taxa from Clade EX was highest on
272 environmental metagenomes ($0.001\% \pm 0.0012$) (figure 1). They were also detected
273 in gut samples ($0.0002\% \pm 0.0005$), albeit with a very low abundance in fecal
274 ($0.0003\% \pm 0.0005$), large intestine ($0.0001\% \pm 0.0002$), stomach ($0.0009\% \pm$
275 0.0006) metagenomes (figure 2). Given their low abundances, further analysis is
276 focused on the FL and HA clades.

277 The aggregated abundance of Clades FL and HA varied across biomes
278 (figure 2). In agreement with their names, HA clade members were enriched in host-
279 associated samples, and FL in non-host samples. The combined abundance of
280 members of Clade FL was higher in samples from environmental biomes ($0.01\% \pm$
281 0.008), although non-zero abundances were observed in digestive system

282 metagenomes (0.008 % \pm 0.015), with some samples containing levels comparable
283 to that of Clade HA (figure 2).

284 The mean abundance of Clade HA in aggregate was higher in metagenomes
285 from gut samples (0.014 % \pm 0.03) compared to environmental biomes (0.004 % \pm
286 0.008). However, among the environmental biomes, non-zero abundances of Clade
287 HA were detected in freshwater (0.002 % \pm 0.003), marine (0.006 % \pm 0.011), saline
288 and alkaline (0.002 % \pm 0.002) and soil (0.004 % \pm 0.003) samples.

289 We further validated the differences in clade abundances across biomes by
290 generating a dendrogram of *Methanomassiliicoccales* taxa using the fold-change
291 enrichment of individual taxa on gut versus environmental biomes, that is, the effect
292 size of their enrichment in either direction. We then compared the structure of this
293 dendrogram with that of the phylogenomic tree and found that they were positively
294 correlated (cophenetic correlation = 0.67, P val. < 0.01).

295 Overall, we observed a low abundance of individual *Methanomassiliicoccales*
296 taxa across all samples, ranging from 0 to 0.15 % (figure 2 and figure S1). The
297 enrichment analysis of individual taxa from Clade FL on diverse biomes showed that
298 while most were significantly enriched in environmental metagenomes, some taxa
299 showed the opposite enrichment. *M. luminyensis* and *Methanomassiliicoccus* sp.
300 UBA386 were not significantly enriched in gut or environmental biomes. “*ca. M.*
301 *intestinalis*” Issoire-Mx1, *Methanomassiliicoccales* archaeon RumEn M1 and
302 *Methanomassiliicoccus* sp. UBA6 were significantly enriched in gut biomes (figure 1),
303 although they were also present in multiple environmental biomes (figure S1).

304 When assessed on a per-taxon basis, the vast majority of Clade HA taxa were
305 significantly enriched in gut samples, with the exception of “*ca. M. termitum*”, which

306 was highly abundant in soil samples from grasslands and water samples from
307 intertidal zones (figure 1).

308

309 ***Genome characteristics and core genes functions differ between***
310 ***Methanomassiliicoccales clades***

311 Given the tendency of clades FL and HA to be enriched in environmental or
312 animal metagenomes, respectively, we searched for genes and genome features
313 linked to putative adaptations of *Methanomassiliicoccales* to an animal gut. For this,
314 we compared 72 genomes from *Methanomassiliicoccales* taxa retrieved from
315 humans, non-human animals and environmental sources.

316 We observed that genomes were more similar to others closely located on the
317 phylogeny for genome GC content, genome length and total gene count (LIPA Adj. P
318 < 0.01 in all cases) (figure 3). To determine whether these features differed between
319 clades, while accounting for the autocorrelation due to evolutionary history, we
320 performed a phylogenetic ANOVA. Clade FL taxa had significantly larger genomes
321 (mean \pm sd: 1985.1 Kb \pm 245.1) than either the clades HA (1318.3 Kb \pm 187.3) or EX
322 (1872.2 Kb \pm 173.8) (phylogenetic ANOVA Adj. P = 0.028). In accord, Clade FL also
323 had the highest gene count (FL: 2153.1 genes \pm 233.7; HA: 1377.7 genes \pm 187.7;
324 EX 1567.0 genes \pm 90.5. Adj. P = 0.025). While non-significant, clades HA and EX
325 taxa tended to have a lower GC content than Clade FL taxa (FL: 59.1 % \pm 4.8; HA:
326 55.8 % \pm 2.8; EX 54.4 % \pm 0.5. Adj. P = 0.6).

327 To compare gene presence and absence across clades, we performed a
328 pangenome analysis. After identification of orthologous gene clusters based on
329 sequence similarity using PanX, we obtained 13,695 clusters, of which 7,312 were
330 present at least once in Clade FL, 6,592 in Clade HA, and 1,833 in Clade EX. A

331 large proportion of gene clusters were of unknown function according to the COG
332 functional classification (38.4 % \pm 4.3); gene clusters of unknown function tended to
333 be small, with only one or two genes (figure S2 A, B). Principal component (PC)
334 analysis of gene cluster presence/absence clearly differentiated clades along PC1.

335 We defined outlier taxa as FL taxa enriched in gut biomes
336 (Methanomassiliicoccales archaeon RumEn M1, Methanomassiliicoccus sp. UBA6,
337 “ca. Methanomassiliicoccus intestinalis” Issoire-Mx1, *Methanomassiliicoccus*
338 *luminyensis* B10 and Methanomassiliicoccus sp. UBA386) and the HA taxon
339 enriched in non-host biomes (“ca. M. termitum”). Outliers mostly clustered with their
340 close relatives, not with the taxa enriched in the same biome (figure 4), with the
341 exception of “ca. Methanomassiliicoccus intestinalis” Issoire-Mx1, which did not
342 cluster with either clade.

343

344 ***Gene clusters enriched in Clade HA evidence adaptation to the gut***
345 ***environment***

346 Because of the small number of genomes that cluster within the Clade EX,
347 and because they are largely absent from animal-associated samples, subsequent
348 analyses focus on comparisons between the clades FL and HA.

349 To identify gene clusters potentially involved in the adaptation of members of
350 Clade HA to a host environment, we compared the gene cluster content between
351 clades. The gene cluster frequency spectrum shows many clusters with a small
352 number of genes: 7,990 (58.3 %) gene clusters were singletons and 2,002 (14.6 %)
353 were doubletons (figure S2 A, B). After removing rare gene clusters by filtering those
354 with near zero variance, we included 2937 clusters, which we then used to perform
355 in phylogenetic ANOVAs. Results reveal 14 gene clusters significantly enriched in

356 HA compared to FL (Adj. $P < 0.1$ in all cases). Three gene clusters are involved in
357 detoxification and xenobiotic metabolism, namely, bile acid:sodium symporter
358 (InterPro accession IPR002657), bleomycin resistance protein (IPR029068) and
359 HAD-superfamily hydrolase (IPR006357). Two clusters are related to shikimate or
360 chorismate metabolism: chorismate mutase II (IPR002701) and prephenate
361 dehydratase (IPR001086). Other annotated clusters include the small unit of
362 exonuclease VII (IPR003761), holliday junction resolvase Hjc (IPR002732), nitrogen
363 regulatory protein PII (IPR015867), xylose isomerase-like protein (IPR013022) and
364 metal-binding domain containing protein (IPR019271). Four had poor or no
365 annotation (table 1).

366

367 ***Genomic adaptations to the gut of members of the FL clade***

368 To determine whether outlier taxa belonging to Clade FL had similar
369 adaptations to the gut as members of Clade HA, we explored gene clusters present
370 in these outliers and in Clade HA but that were rare in other members of Clade FL.
371 We selected gene clusters present in the core genome of Clade HA (i.e. present in
372 >80 % of taxa from this clade, see supplementary results) and present in less than
373 half of FL taxa. A total of 15 gene clusters were obtained, most of them encoded by
374 only one of the outlier taxa. Two gene clusters, ferrous iron transport proteins A and
375 B (IPR030389 and IPR007167), were present in three of the outliers
376 (Methanomassiliicoccus luminyensis B10, “*candidatus* Methanomassiliicoccus
377 intestinalis” Issoire-Mx1 and Methanomassiliicoccales archaeon RumEn M1). Other
378 clusters detected in more than one outlier included an uncharacterised membrane
379 protein (IPR005182, in Methanomassiliicoccus sp. UBA6 and
380 Methanomassiliicoccales archaeon RumEn M1), a putative nickel-responsive

381 regulator (IPR014864, in *Methanomassiliicoccus luminyensis* B10 and
382 *Methanomassiliicoccus* sp UBA386), and an ABC transporter (IPR037294, in
383 *Methanomassiliicoccus luminyensis* B10 and *Methanomassiliicoccus* sp UBA386).
384 The remaining gene clusters, detected once, corresponded to transcriptional
385 regulators or proteins of unknown function.

386

387 ***The genomes of taxa from clades HA and FL encode distinct repertoires of***
388 ***adhesion proteins***

389 We compared between FL and HA clades two large groups of membrane
390 proteins involved in adhesion: eukaryote-like proteins (ELPs), a series of protein
391 families involved in microbial adherence to its host (38), and adhesin-like proteins
392 (ALPs), a class of proteins hypothesized to be involved in the microbe-microbe
393 interactions of *Methanobacteriales* in the gut (13). We aggregated the counts of gene
394 clusters annotated as the ALP and ELP classes, and performed phylogenetic
395 ANOVA. This analysis showed that members of each clade tended to encode a
396 different repertoire of adhesion proteins (figure 3). Taxa from Clade HA had a higher
397 mean count of tetratricopeptide repeats (Mean \pm SD count; HA: 16.30 \pm 06.56, FL:
398 9.55 \pm 1.70), Sel1 repeats (HA: 9.32 \pm 5.69, FL: 0.35 \pm 1.35), Listeria-Bacteroides
399 repeats (HA: 3.68 \pm 3.76, FL: 1.65 \pm 5.78) and leucine-rich repeats (HA: 1.5 \pm 2.15, FL:
400 1.1 \pm 2.02) than FL taxa, although we did not observe significant differences in their
401 frequency (Adj. P > 0.1 in all cases). Conversely, ALPs (FL: 2.25 \pm 1.48, HA:
402 0.14 \pm 0.61) and Ig-like domains, (FL: 1.55 \pm 1.32, HA: 0.20 \pm 0.53) tended to be more
403 abundant in the genomes of members of Clade FL.

404 Interestingly, outlier taxa from Clade FL had gene counts of several of the
405 adhesion factors higher than the mean of their own clade and more characteristic of

406 clade HA. In some cases, the gene counts were higher than the mean for Clade HA.
407 These included Listeria-Bacteroides repeats (gene cluster count - *M. luminyensis*: 2,
408 “ca. *M. intestinalis*” Issoire-Mx1: 26, Methanomassiliicoccales archaeon RumEn M1:
409 2), Sel1 repeats (*M. luminyensis*: 1, “ca. *M. intestinalis*” Issoire-Mx1: 6), and leucine-
410 rich repeats (*M. luminyensis*: 5, “ca. *M. intestinalis*” Issoire-Mx1: 7).

411

412 ***Methanomassiliicoccales* taxa cooccur with each other, with other Archaea,**
413 **and with TMA producing bacteria in the human gut**

414 We characterized the distribution of *Methanomassiliicoccales* across a
415 collection of human gut metagenomes derived from 34 studies. Together, the
416 combined 4472 samples represented people from 22 countries, resulting in 35
417 unique datasets (*i.e.*, study-country combination). Across the whole set, we detected
418 just two genera: *Methanomassiliicoccus* (Clade FL) and “ca. *Methanomethylophilus*”
419 (Clade HA), both rare members of the human gut microbiota (figure 5). “ca.
420 *Methanomethylophilus*” was detectable in 19 out of 35 datasets; on these 19
421 datasets it had a prevalence ranging from 0.5 % to 41.7 %, and mean abundance
422 ranged from 4.8×10^{-6} % to 2.2×10^{-2} %. Similarly, *Methanomassiliicoccus* was
423 detectable in 22 of the 35 datasets; on the 22 datasets it had a prevalence range of 1
424 % to 25.7 % and a mean abundance range of 1.5×10^{-5} % to 1.0×10^{-2} % (table S4).

425 We tested associations of these two genera with age, sex and westernization
426 status of the subjects using linear mixed models that included the dataset and
427 country as random effects. Subjects from non-westernized countries had a
428 significantly higher prevalence of “ca. *Methanomethylophilus*” (mean prevalence \pm
429 SD: Non-westernized = 8.9 % \pm 28.5, Westernized 1.1 % \pm 10.3; P Adj. = 0.002).
430 Westernized individuals were more likely to harbor higher *Methanomassiliicoccus*,

431 although differences were not significant (Non-westernized = 3.9 % \pm 19.4,
432 Westernized 5.0 % \pm 21.7; P Adj. > 0.1). The age and sex of the individuals did not
433 explain variance in the prevalence or abundance of either genus (Adj. P > 0.1 in all
434 cases).

435 To identify other microbial taxa positively associated with members of
436 *Methanomassiliicoccales* in the human gut, we calculated a network of positively
437 associated microorganisms (*i.e.* coabundant taxa) across samples (ρ > 0.1 in all
438 cases) (53). In addition, we determined which taxa were present with members of
439 *Methanomassiliicoccales* more than expected by chance (*i.e.* cooccurring taxa)
440 relative to a permuted null model (43). Results showed that both “*ca.*
441 *Methanomethylophilus*” and *Methanomassiliicoccus* were part of the same
442 coabundance network, together with a third archaeal genus, *Methanoculleus* (order
443 *Methanomicrobiales*). We did not find evidence of positive or negative abundance
444 associations of either *Methanomassiliicoccales* genus with *Methanobrevibacter*.
445 Cooccurrence analysis showed a random association pattern between these taxa (P
446 val. > 0.05 for both “*ca.* *Methanomethylophilus*” and *Methanomassiliicoccus*),
447 indicating that their ecological niches do not overlap with *Methanobrevibacter*.

448 Analysis of the combined network of “*ca.* *Methanomethylophilus*” and
449 *Methanomassiliicoccus* revealed a large overlap between taxa associated with either
450 genus (figure 6): out of 119 taxa in the network, 86 (72.3 %) were associated with
451 both. Moreover, 51 taxa (42.9 %) also had a significant positive cooccurrence pattern
452 with both genera (P val. < 0.05 in all cases). Most bacterial members of this network
453 had an overall low relative abundance. Interestingly, they included several taxa
454 whose genomes contain genes encoding enzymes involved in TMA production,

455 including *Bacteroides*, *Campylobacter*, *Yokenella*, *Mobiluncus*, *Proteus*, *Providencia*
456 and *Edwardsiella* (54).

457

458 ***Abundance of Methanomassiliicoccales is not concordant in monozygotic or***
459 ***dizygotic human twins***

460 To evaluate whether host genetics influences the abundance of
461 *Methanomassiliicoccales* in the human gut, we compared the intraclass correlation
462 coefficient (ICC) of their abundances at the genus level using a set of 153
463 monozygotic (MZ) and 200 dizygotic (DZ) twin pairs from the TwinsUK cohort. As
464 control, we first compared the mean ICC across all taxa between MZ and DZ twins,
465 and found that ICC_{MZ} (0.1) was significantly higher than ICC_{DZ} (0.03) (P val. < 0.01).
466 In addition, we assessed the ICC values of bacterial (*Christensenella*,
467 *Faecalibacterium* and *Bifidobacterium*) and archaeal (*Methanobrevibacter*), and
468 consistently found a higher correlation on MZ compared to DZ twins (table S5). We
469 were only able to assess ICC values of *Methanomassiliicoccus*, as it was the only
470 *Methanomassiliicoccales* detected in the twins with a prevalence (8.64 %) above the
471 5 % cutoff (see methods). We did not detect a significant concordance between the
472 abundances of *Methanomassiliicoccus* in MZ ($ICC_{MZ} = 0.004$, Adj. P = 0.59) or in DZ
473 twins ($ICC_{DZ} = 0.017$, Adj. P = 0.71). Given the low abundance of
474 *Methanomassiliicoccales* taxa, we performed a sensitivity analysis using samples
475 with a high sequencing depth (>12 million reads/sample), however, we did not
476 observe differences in the abundance and prevalence of the
477 *Methanomassiliicoccales* genera nor the ICC estimates (not shown).

478

479 Discussion

480 While the source of the members of the *Methanomassiliicoccales* has been
481 noted in previous surveys of single markers such as 16S rRNA and mcrA genes (9,
482 10), here we searched metagenomes from host associated and environmental
483 samples for their relative abundances. Overall, the HA taxa were enriched in host
484 associated samples and the FL taxa in environmental samples; intriguingly, all taxa
485 regardless of clade were detected in both biomes. This suggests that members of
486 the order *Methanomassiliicoccales* are generalists with an overall habitat preference
487 according to clade, although there were some exceptions to the general pattern. We
488 show that members of *Methanomassiliicoccales* use many of the same adaptations
489 to the gut as other methanogens. These adaptations include genome reduction, and
490 genes involved in the shikimate pathway and bile resistance. In addition, gut-
491 enriched taxa possess a distinct repertoire of genes encoding adhesion factors. We
492 observed that potential adaptations to the gut differed by clade, not preferred habitat,
493 indicating convergence on a shared niche through different genomic solutions. In the
494 human gut, *Methanomassiliicoccales* taxa correlated with TMA-producing bacteria,
495 rather than host genetics or other host factors.

496 For members of the HA clade, adaptations to life in the gut included an
497 enrichment of genes involved in bile acid transport, efflux pumps, and hydrolases,
498 which play a role in tolerance to these compounds in the gastrointestinal tract (55).
499 This adaptation is also shared with other members of the gut microbiota, including
500 *Methanobacteriales*: *M. smithii* and *M. stadtmanae* are resistant to bile salts (2, 3).
501 Other gene clusters with known function enriched in Clade HA are involved in
502 metabolism of shikimate and chorismate. The shikimate pathway is involved in the
503 synthesis of aromatic amino acids in plants and microbes, but is absent in mammals.

504 Shikimate metabolism is carried out by archaeal (56) and bacterial (57, 58) members
505 of the animal gut microbiota, and was reported as one of the most conserved
506 metabolic modules in a large-scale gene catalogue from the human gut (59).
507 Derivatives from the aromatic amino acids are known to be bioactive in the mammal
508 host (60).

509 In addition, members of the HA clade had a particular set of adhesion factors,
510 known to be involved in the maintenance of syntrophic relationships of the
511 methanogens with bacterial (12, 61) or eukaryotic (62) microorganisms. Two groups
512 of adhesion factors, proteins containing Sel1 domains and Listeria-Bacteroides
513 repeats, have been previously studied on *Methanomassiliicoccales* taxa retrieved
514 from the gut (11, 52). Our assessment of these factors in the broader context of the
515 order *Methanomassiliicoccales* showed that these two groups of proteins are
516 characteristic of Clade HA rather than FL, with the exception of the outlier taxa.
517 Indeed, while the repertoire of ELPs and ALPs differs between HA and FL taxa, it
518 was similar between species inhabiting the gut regardless of their clade.

519 In contrast, members of Clade FL appear to be generalists that colonized the
520 animal gut independently from the HA clade. It has been previously noted that *M.*
521 *luminyensis*, an outlier from Clade FL, could have a facultative association to the
522 animal gut. It possesses genes involved in nitrogen fixation, oxidative stress (11) and
523 mercury methylation (52), which are common in soil microorganisms but rare in
524 members of the gut microbiota (63). In accord, we observed that members of Clade
525 FL are widespread and abundant on soil, water and gut metagenomes, with a
526 preference for environmental biomes. Similarities in ELP content between gut-
527 dwelling taxa from both clades indicate that interaction with the host or other
528 members of the gut microbiota might be a key factor in the adaptation of these

529 methanogens.

530 Analysis of the gene content of outlier taxa from Clade FL showed that they
531 tended to be more similar to members of their own clade than to taxa from Clade HA,
532 with the exception of “*ca. M. intestinalis*” Issoire-Mx1, which was distinct from either
533 Clade FL and HA. In addition there was little overlap in gene clusters commonly
534 observed in Clade HA and outlier taxa from Clade FL, with the exception of the
535 adhesion factors discussed below. These observations support the hypothesis that
536 colonization of animal guts by members of *Methanomassiliicoccales* occurred in two
537 independent events (11, 52), and suggests that there is not one solution to life in the
538 gut for these *Archaea*, as members from two clades seem to have solved the
539 problem with a different set of adaptations.

540 Characterization of the abundance of *Methanomassiliicoccales* across human
541 populations showed members of this group are rare in the microbiota of healthy
542 adults. We did not detect them in all the studied populations, and when detected,
543 they had low prevalence and abundance. Nevertheless, this analysis allowed us to
544 assess whether *Archaea* in the human gut are mutually exclusive. We observed
545 positive correlations of “*ca. Methanomethylophilus*” and *Methanomassiliicoccus* with
546 each other and with *Methanoculleus*, another rare archaeal member of the gut
547 microbiota (64). We did not find evidence of association between members of
548 *Methanomassiliicoccales* and *Methanobrevibacter*, positive or otherwise, confirming
549 the previous report that these methanogens are not mutually exclusive (46);
550 abundance of H₂ in the gut, together with differences in other substrate utilization,
551 might result in non-overlapping niches (65).

552 While genus *Methanobrevibacter* has been consistently found to have a
553 moderate heritability the TwinsUK (19, 46, 66) and other cohorts (48, 67), it was not

554 the case for members of *Methanomassiliicoccales*. Similar to humans, methane
555 production (68) and abundance of *Methanobrevibacter* (69) are also heritable in
556 bovine cattle, but not *Methanomassiliicoccales* taxa (69). Thus, host genetics might
557 be linked to particular taxa and methanogenesis pathways, not to all *Archaea* or
558 methane production as a whole.

559 Genera “ca. *Methanomethylophilus*” and *Methanomassiliicoccus* cooccur with
560 TMA-producing bacteria (54), further supporting their potential use as a way of
561 targeting intestinal TMA (70). The exact nature of the ecological relationships each of
562 these taxa establishes with other members of the microbiome remains to be
563 elucidated. In a facilitation scenario between the methanogens and H₂- and TMA-
564 producers, freely available TMA and H₂ required for methylotrophic methanogenesis
565 could be utilized by *Methanomassiliicoccales* taxa (71), without cost to the producer.
566 Alternatively, the methanogens could establish syntrophic interactions with other
567 microorganisms, whereby the consumption of these metabolites is also beneficial to
568 the producer (71).

569 The present study extends our understanding of the order
570 *Methanomassiliicoccales* by revealing genomic adaptations to life in the gut by
571 members of both clades that make up this group. Furthermore, the positive
572 correlation between the relative abundances of these TMA-utilizing archaea with
573 TMA-producing bacteria in the gut is a first step towards understanding how they
574 may be harnessed for therapeutic management of gut TMA levels in the context of
575 cardiovascular disease.

576

577 **Acknowledgements**

578 This work was supported by the Max Planck Society. We thank EMBO, the

579 organizers and participants of the Bioinformatics and genome analyses course held
580 at the Fondazione Edmund Mach in San Michele all'Adige, Italy, for sponsoring the
581 attendance of J.dIC-Z and for their feedback. We are also grateful to Daphne Welter,
582 Jessica Sutter and Albane Ruaud for the fruitful discussions and comments. The
583 study also received support from the National Institute for Health Research (NIHR)
584 BioResource Clinical Research Facility and Biomedical Research Centre based at
585 Guy's and St Thomas' NHS Foundation Trust and King's College London. We
586 declare no competing interests.

587

588 **References**

- 589 1. Borrel G, Brugère J-F, Gribaldo S, Schmitz RA, Moissl-Eichinger C. 2020. The host-
590 associated archaeome. *Nat Rev Microbiol*.
- 591 2. Miller TL, Wolin MJ. 1982. Enumeration of *Methanobrevibacter smithii* in human feces.
592 *Arch Microbiol* 131:14–18.
- 593 3. Miller TL, Wolin MJ. 1985. *Methanosphaera stadtmaniae* gen. nov., sp. nov.: a species
594 that forms methane by reducing methanol with hydrogen. *Arch Microbiol* 141:116–122.
- 595 4. Horz H-P, Conrads G. 2010. The discussion goes on: What is the role of Euryarchaeota
596 in humans? *Archaea* 2010:967271.
- 597 5. Moissl-Eichinger C, Pausan M, Taffner J, Berg G, Bang C, Schmitz RA. 2018. *Archaea*
598 Are Interactive Components of Complex Microbiomes. *Trends Microbiol* 26:70–85.
- 599 6. Borrel G, Harris HMB, Tottey W, Mihajlovski A, Parisot N, Peyretailade E, Peyret P,
600 Gribaldo S, O'Toole PW, Brugère J-F. 2012. Genome Sequence of “*Candidatus*
601 *Methanomethylophilus alvus*” Mx1201, a Methanogenic Archaeon from the Human Gut
602 Belonging to a Seventh Order of Methanogens. *J Bacteriol* 194:6944–6945.

- 603 7. Borrel G, Harris HMB, Parisot N, Gaci N, Tottey W, Mihajlovski A, Deane J, Gribaldo S,
604 Bardot O, Peyretailade E, Peyret P, O'Toole PW, Brugère J-F. 2013. Genome
605 Sequence of “Candidatus Methanomassiliicoccus intestinalis” Issoire-Mx1, a Third
606 Thermoplasmatales-Related Methanogenic Archaeon from Human Feces. *Genome*
607 *Announc* 1:e00453–13.
- 608 8. Dridi B, Fardeau M-L, Ollivier B, Raoult D, Drancourt M. 2012. *Methanomassiliicoccus*
609 *luminyensis* gen. nov., sp. nov., a methanogenic archaeon isolated from human faeces.
610 *Int J Syst Evol Microbiol* 62:1902–1907.
- 611 9. Söllinger A, Schwab C, Weinmaier T, Loy A, Tveit AT, Schleper C, Urich T. 2016.
612 Phylogenetic and genomic analysis of Methanomassiliicoccales in wetlands and animal
613 intestinal tracts reveals clade-specific habitat preferences. *FEMS Microbiol Ecol*
614 92:fiv149.
- 615 10. Speth DR, Orphan VJ. 2018. Metabolic marker gene mining provides insight in global
616 diversity and, coupled with targeted genome reconstruction, sheds further light on
617 metabolic potential of the. *PeerJ* 6:e5614.
- 618 11. Borrel G, Parisot N, Harris HMB, Peyretailade E, Gaci N, Tottey W, Bardot O, Raymann
619 K, Gribaldo S, Peyret P, O'Toole PW, Brugère J-F. 2014. Comparative genomics
620 highlights the unique biology of Methanomassiliicoccales, a Thermoplasmatales-related
621 seventh order of methanogenic archaea that encodes pyrrolysine. *BMC Genomics*
622 15:679.
- 623 12. Samuel BS, Hansen EE, Manchester JK, Coutinho PM, Henrissat B, Fulton R, Latreille
624 P, Kim K, Wilson RK, Gordon JI. 2007. Genomic and metabolic adaptations of
625 *Methanobrevibacter smithii* to the human gut. *Proc Natl Acad Sci U S A* 104:10643–
626 10648.
- 627 13. Hansen EE, Lozupone CA, Rey FE, Wu M, Guruge JL, Narra A, Goodfellow J, Zaneveld

- 628 JR, McDonald DT, Goodrich JA, Heath AC, Knight R, Gordon JI. 2011. Pan-genome of
629 the dominant human gut-associated archaeon, *Methanobrevibacter smithii*, studied in
630 twins. *Proc Natl Acad Sci U S A* 108 Suppl 1:4599–4606.
- 631 14. Söllinger A, Urich T. 2019. Methylophilic methanogens everywhere - physiology and
632 ecology of novel players in global methane cycling. *Biochem Soc Trans* 47:1895–1907.
- 633 15. Brown JM, Hazen SL. 2018. Microbial modulation of cardiovascular disease. *Nat Rev*
634 *Microbiol* 16:171–181.
- 635 16. Geng J, Yang C, Wang B, Zhang X, Hu T, Gu Y, Li J. 2018. Trimethylamine N-oxide
636 promotes atherosclerosis via CD36-dependent MAPK/JNK pathway. *Biomed*
637 *Pharmacother* 97:941–947.
- 638 17. Wang Z, Roberts AB, Buffa JA, Levison BS, Zhu W, Org E, Gu X, Huang Y, Zamanian-
639 Daryoush M, Culley MK, DiDonato AJ, Fu X, Hazen JE, Krajcik D, DiDonato JA, Lusis
640 AJ, Hazen SL. 2015. Non-lethal Inhibition of Gut Microbial Trimethylamine Production
641 for the Treatment of Atherosclerosis. *Cell* 163:1585–1595.
- 642 18. Brugère J-F, Borrel G, Gaci N, Tottey W, O'Toole PW, Malpuech-Brugère C. 2014.
643 Archaeobiotics: proposed therapeutic use of archaea to prevent trimethylaminuria and
644 cardiovascular disease. *Gut Microbes* 5:5–10.
- 645 19. Xie H, Guo R, Zhong H, Feng Q, Lan Z, Qin B, Ward KJ, Jackson MA, Xia Y, Chen X,
646 Chen B, Xia H, Xu C, Li F, Xu X, Al-Aama JY, Yang H, Wang J, Kristiansen K, Wang J,
647 Steves CJ, Bell JT, Li J, Spector TD, Jia H. 2016. Shotgun Metagenomics of 250 Adult
648 Twins Reveals Genetic and Environmental Impacts on the Gut Microbiome. *Cell*
649 *systems* 3:572–584.e3.
- 650 20. Parks DH, Imelfort M, Skennerton CT, Hugenholtz P, Tyson GW. 2015. CheckM:
651 assessing the quality of microbial genomes recovered from isolates, single cells, and
652 metagenomes. *Genome Res* 25:1043–1055.

- 653 21. Seemann T. 2014. Prokka: rapid prokaryotic genome annotation. *Bioinformatics*
654 30:2068–2069.
- 655 22. Segata N, Börnigen D, Morgan XC, Huttenhower C. 2013. PhyloPhlAn is a new method
656 for improved phylogenetic and taxonomic placement of microbes. *Nat Commun* 4:2304.
- 657 23. Katoh K, Standley DM. 2013. MAFFT multiple sequence alignment software version 7:
658 improvements in performance and usability. *Mol Biol Evol* 30:772–780.
- 659 24. Stamatakis A. 2014. RAxML version 8: a tool for phylogenetic analysis and post-
660 analysis of large phylogenies. *Bioinformatics* 30:1312–1313.
- 661 25. Letunic I, Bork P. 2016. Interactive tree of life (iTOL) v3: an online tool for the display
662 and annotation of phylogenetic and other trees. *Nucleic Acids Res* 44:W242–5.
- 663 26. Mitchell AL, Scheremetjew M, Denise H, Potter S, Tarkowska A, Qureshi M, Salazar
664 GA, Pesseat S, Boland MA, Hunter FMI, Ten Hoopen P, Alako B, Amid C, Wilkinson DJ,
665 Curtis TP, Cochrane G, Finn RD. 2018. EBI Metagenomics in 2017: enriching the
666 analysis of microbial communities, from sequence reads to assemblies. *Nucleic Acids*
667 *Res* 46:D726–D735.
- 668 27. Breitwieser FP, Baker DN, Salzberg SL. 2018. KrakenUniq: confident and fast
669 metagenomics classification using unique k-mer counts. *Genome Biol* 19:198.
- 670 28. R Core Team. 2018. R: A Language and Environment for Statistical Computing. R
671 Foundation for Statistical Computing, Vienna, Austria.
- 672 29. Love MI, Huber W, Anders S. 2014. Moderated estimation of fold change and dispersion
673 for RNA-seq data with DESeq2. *Genome Biol* 15:550.
- 674 30. Paradis E, Claude J, Strimmer K. 2004. APE: Analyses of Phylogenetics and Evolution
675 in R language. *Bioinformatics* 20:289–290.

- 676 31. Ding W, Baumdicker F, Neher RA. 2018. panX: pan-genome analysis and exploration.
677 Nucleic Acids Res 46:e5.
- 678 32. Finn RD, Attwood TK, Babbitt PC, Bateman A, Bork P, Bridge AJ, Chang H-Y,
679 Dosztányi Z, El-Gebali S, Fraser M, Gough J, Haft D, Holliday GL, Huang H, Huang X,
680 Letunic I, Lopez R, Lu S, Marchler-Bauer A, Mi H, Mistry J, Natale DA, Necci M, Nuka
681 G, Orengo CA, Park Y, Pesseat S, Piovesan D, Potter SC, Rawlings ND, Redaschi N,
682 Richardson L, Rivoire C, Sangrador-Vegas A, Sigrist C, Sillitoe I, Smithers B, Squizzato
683 S, Sutton G, Thanki N, Thomas PD, Tosatto SCE, Wu CH, Xenarios I, Yeh L-S, Young
684 S-Y, Mitchell AL. 2017. InterPro in 2017-beyond protein family and domain annotations.
685 Nucleic Acids Res 45:D190–D199.
- 686 33. Huerta-Cepas J, Forslund K, Coelho LP, Szklarczyk D, Jensen LJ, von Mering C, Bork
687 P. 2017. Fast Genome-Wide Functional Annotation through Orthology Assignment by
688 eggNOG-Mapper. Mol Biol Evol 34:2115–2122.
- 689 34. Buchfink B, Xie C, Huson DH. 2015. Fast and sensitive protein alignment using
690 DIAMOND. Nat Methods 12:59–60.
- 691 35. Keck F, Rimet F, Bouchez A, Franc A. 2016. phylosignal: an R package to measure,
692 test, and explore the phylogenetic signal. Ecol Evol 6:2774–2780.
- 693 36. Snipen L, Liland KH. 2015. micropan: an R-package for microbial pan-genomics. BMC
694 Bioinformatics 16:79.
- 695 37. Revell LJ. 2012. phytools: an R package for phylogenetic comparative biology (and
696 other things): phytools: R package. Methods Ecol Evol 3:217–223.
- 697 38. Alex A, Antunes A. 2018. Genus-wide comparison of Pseudovibrio bacterial genomes
698 reveal diverse adaptations to different marine invertebrate hosts. PLoS One
699 13:e0194368.

- 700 39. Pasolli E, Schiffer L, Manghi P, Renson A, Obenchain V, Truong DT, Beghini F, Malik F,
701 Ramos M, Dowd JB, Huttenhower C, Morgan M, Segata N, Waldron L. 2017.
702 Accessible, curated metagenomic data through ExperimentHub. *Nat Methods* 14:1023–
703 1024.
- 704 40. Wood DE, Lu J, Langmead B. 2019. Improved metagenomic analysis with Kraken 2.
705 *Genome Biol* 20:257.
- 706 41. Lu J, Breitwieser FP, Thielen P, Salzberg SL. 2017. Bracken: estimating species
707 abundance in metagenomics data. *PeerJ Computer Science* 3:e104.
- 708 42. de la Cuesta-Zuluaga J, Ley RE, Youngblut ND. 2020. Struo: a pipeline for building
709 custom databases for common metagenome profilers. *Bioinformatics* 36:2314–2315.
- 710 43. Griffith DM, Veech JA, Marsh CJ. 2016. cooccur : Probabilistic Species Co-Occurrence
711 Analysis in R. *J Stat Softw* 69:1–17.
- 712 44. Quinn TP, Richardson MF, Lovell D, Crowley TM. 2017. propr: An R-package for
713 Identifying Proportionally Abundant Features Using Compositional Data Analysis. *Sci*
714 *Rep* 7:16252.
- 715 45. Bates D, Mächler M, Bolker B, Walker S. 2015. Fitting Linear Mixed-Effects Models
716 Using lme4. *J Stat Softw* 67:1–48.
- 717 46. Goodrich JK, Waters JL, Poole AC, Sutter JL, Koren O, Blekhman R, Beaumont M, Van
718 Treuren W, Knight R, Bell JT, Spector TD, Clark AG, Ley RE. 2014. Human genetics
719 shape the gut microbiome. *Cell* 159:789–799.
- 720 47. Visconti A, Le Roy CI, Rosa F, Rossi N, Martin TC, Mohny RP, Li W, de Rinaldis E,
721 Bell JT, Venter JC, Nelson KE, Spector TD, Falchi M. 2019. Interplay between the
722 human gut microbiome and host metabolism. *Nat Commun* 10:4505.
- 723 48. Goodrich JK, Davenport ER, Clark AG, Ley RE. 2017. The Relationship Between the

- 724 Human Genome and Microbiome Comes into View. *Annu Rev Genet* 51:413–433.
- 725 49. Paul K, Nonoh JO, Mikulski L, Brune A. 2012. “Methanoplasmatales,”
726 Thermoplasmatales-related archaea in termite guts and other environments, are the
727 seventh order of methanogens. *Appl Environ Microbiol* 78:8245–8253.
- 728 50. Borrel G, O’Toole PW, Harris HMB, Peyret P, Brugère J-F, Gribaldo S. 2013.
729 Phylogenomic data support a seventh order of Methylophilic methanogens and
730 provide insights into the evolution of Methanogenesis. *Genome Biol Evol* 5:1769–1780.
- 731 51. Parks DH, Rinke C, Chuvochina M, Chaumeil P-A, Woodcroft BJ, Evans PN,
732 Hugenholtz P, Tyson GW. 2017. Recovery of nearly 8,000 metagenome-assembled
733 genomes substantially expands the tree of life. *Nat Microbiol* 2:1533–1542.
- 734 52. Borrel G, McCann A, Deane J, Neto MC, Lynch DB, Brugère J-F, O’Toole PW. 2017.
735 Genomics and metagenomics of trimethylamine-utilizing Archaea in the human gut
736 microbiome. *ISME J* 11:2059–2074.
- 737 53. Quinn TP, Erb I, Richardson MF, Crowley TM. 2018. Understanding sequencing data as
738 compositions: an outlook and review. *Bioinformatics* 34:2870–2878.
- 739 54. Fennema D, Phillips IR, Shephard EA. 2016. Trimethylamine and Trimethylamine N-
740 Oxide, a Flavin-Containing Monooxygenase 3 (FMO3)-Mediated Host-Microbiome
741 Metabolic Axis Implicated in Health and Disease. *Drug Metab Dispos* 44:1839–1850.
- 742 55. Begley M, Gahan CGM, Hill C. 2005. The interaction between bacteria and bile. *FEMS*
743 *Microbiol Rev* 29:625–651.
- 744 56. Hovey R, Lenters S, Ehrenreich A, Salmon K, Saba K, Gottschalk G, Gunsalus RP,
745 Deppenmeier U. 2005. DNA microarray analysis of *Methanosarcina mazei* Gö1 reveals
746 adaptation to different methanogenic substrates. *Mol Genet Genomics* 273:225–239.
- 747 57. Kamke J, Kittelmann S, Soni P, Li Y, Tavendale M, Ganesh S, Janssen PH, Shi W,

- 748 Froula J, Rubin EM, Attwood GT. 2016. Rumen metagenome and metatranscriptome
749 analyses of low methane yield sheep reveals a Sharpea-enriched microbiome
750 characterised by lactic acid formation and utilisation. *Microbiome* 4:56.
- 751 58. LeBlanc JG, Milani C, de Giori GS, Sesma F, van Sinderen D, Ventura M. 2013.
752 Bacteria as vitamin suppliers to their host: a gut microbiota perspective. *Curr Opin*
753 *Biotechnol* 24:160–168.
- 754 59. Almeida A, Nayfach S, Boland M, Strozzi F, Beracochea M, Shi ZJ, Pollard KS,
755 Sakharova E, Parks DH, Hugenholtz P, Segata N, Kyrpides NC, Finn RD. 2020. A
756 unified catalog of 204,938 reference genomes from the human gut microbiome. *Nat*
757 *Biotechnol* 49:55.
- 758 60. Sridharan GV, Choi K, Klemashevich C, Wu C, Prabakaran D, Pan LB, Steinmeyer S,
759 Mueller C, Yousofshahi M, Alaniz RC, Lee K, Jayaraman A. 2014. Prediction and
760 quantification of bioactive microbiota metabolites in the mouse gut. *Nat Commun*
761 5:5492.
- 762 61. Ruaud A, Esquivel-Elizondo S, de la Cuesta-Zuluaga J, Waters JL, Angenent LT,
763 Youngblut ND, Ley RE. 2020. Syntrophy via interspecies H₂ transfer between and
764 underlies their global cooccurrence in the human gut. *MBio* 11:e03235–19.
- 765 62. Ng F, Kittelmann S, Patchett ML, Attwood GT, Janssen PH, Rakonjac J, Gagic D. 2016.
766 An adhesin from hydrogen-utilizing rumen methanogen *Methanobrevibacter*
767 *ruminantium* M1 binds a broad range of hydrogen-producing microorganisms. *Environ*
768 *Microbiol* 18:3010–3021.
- 769 63. Podar M, Gilmour CC, Brandt CC, Soren A, Brown SD, Crable BR, Palumbo AV,
770 Somenahally AC, Elias DA. 2015. Global prevalence and distribution of genes and
771 microorganisms involved in mercury methylation. *Sci Adv* 1:e1500675.
- 772 64. Horz H-P. 2015. Archaeal Lineages within the Human Microbiome: Absent, Rare or

- 773 Elusive? *Life* 5:1333–1345.
- 774 65. Feldewert C, Lang K, Brune A. 2020. The hydrogen threshold of obligately methyl-
775 reducing methanogens. *FEMS Microbiol Lett* fnaa137.
- 776 66. Goodrich JK, Davenport ER, Beaumont M, Jackson MA, Knight R, Ober C, Spector TD,
777 Bell JT, Clark AG, Ley RE. 2016. Genetic Determinants of the Gut Microbiome in UK
778 Twins. *Cell Host Microbe* 19:731–743.
- 779 67. Kurilshikov A, Medina-Gomez C, Bacigalupe R, Radjabzadeh D, Wang J, Demirkan A,
780 Le Roy CI, Raygoza Garay JA, Finnicum CT, Liu X, Zhernakova DV, Bonder MJ,
781 Hansen TH, Frost F, Rühlemann MC, Turpin W, Moon J-Y, Kim H-N, Lüll K, Barkan E,
782 Shah SA, Fornage M, Szopinska-Tokov J, Wallen ZD, Borisevich D, Agreus L,
783 Andreasson A, Bang C, Bedrani L, Bell JT, Bisgaard H, Boehnke M, Boomsma DI, Burk
784 RD, Claringbould A, Croitoru K, Davies GE, van Duijn CM, Duijts L, Falony G, Fu J, van
785 der Graaf A, Hansen T, Homuth G, Hughes DA, Ijzerman RG, Jackson MA, Jaddoe
786 VWV, Joossens M, Jørgensen T, Keszthelyi D, Knight R, Laakso M, Laudes M, Launer
787 LJ, Lieb W, Lusic AJ, Masclee AAM, Moll HA, Mujagic Z, Qibin Q, Rothschild D, Shin H,
788 Sørensen SJ, Steves CJ, Thorsen J, Timpson NJ, Tito RY, Vieira-Silva S, Völker U,
789 Völzke H, Vösa U, Wade KH, Walter S, Watanabe K, Weiss S, Weiss FU, Weissbrod O,
790 Westra H-J, Willemsen G, Payami H, Jonkers DMAE, Vasquez AA, de Geus EJC,
791 Meyer KA, Stockholm J, Segal E, Org E, Wijmenga C, Kim H-L, Kaplan RC, Spector TD,
792 Uitterlinden AG, Rivadeneira F, Franke A, Lerch MM, Franke L, Sanna S, D'Amato M,
793 Pedersen O, Paterson AD, Kraaij R, Raes J, Zhernakova A. 2020. Genetics of human
794 gut microbiome composition. *bioRxiv*;2020.06.26.173724v1. *Genetics*. *bioRxiv*.
- 795 68. Roehe R, Dewhurst RJ, Duthie C-A, Rooke JA, McKain N, Ross DW, Hyslop JJ,
796 Waterhouse A, Freeman TC, Watson M, Wallace RJ. 2016. Bovine Host Genetic
797 Variation Influences Rumen Microbial Methane Production with Best Selection Criterion
798 for Low Methane Emitting and Efficiently Feed Converting Hosts Based on

- 799 Metagenomic Gene Abundance. *PLoS Genet* 12:e1005846.
- 800 69. Difford GF, Plichta DR, Løvendahl P, Lassen J, Noel SJ, Højberg O, Wright A-DG, Zhu
801 Z, Kristensen L, Nielsen HB, Guldbbrandtsen B, Sahana G. 2018. Host genetics and the
802 rumen microbiome jointly associate with methane emissions in dairy cows. *PLoS Genet*
803 14:e1007580.
- 804 70. Hania WB, Ballet N, Vandekerckove P, Ollivier B, O'Toole PW, Brugère J-F. 2017.
805 Archaeobiotics: Archaea as Pharmabiotics for Treating Chronic Disease in Humans?, p.
806 42–62. *In* Sghaier, H, Najjari, A, Ghedira, K (eds.), *Archaea - New Biocatalysts, Novel*
807 *Pharmaceuticals and Various Biotechnological Applications*. InTech.
- 808 71. Douglas AE. 2020. The microbial exometabolome: ecological resource and architect of
809 microbial communities. *Philos Trans R Soc Lond B Biol Sci* 375:20190250.

810 **Figure and table legends**

811 *Figure legends*

812 **Figure 1. The order *Methanomassiliicoccales* forms two large clades that**

813 **loosely follow the source of isolation.** A maximum likelihood phylogeny of

814 concatenated single-copy marker genes. The gray triangle corresponds to

815 *Thermoplasma acidophilum*, *Picrophilus oshimae*, *Ferroplasma acidarmanus*,

816 *Acidiplasma aeolicum* and *Cuniculiplasma divulgatum*; outgroup taxa from class

817 *Thermoplasmata*. Black circles indicate bootstrap values of > 80 (of 100 bootstrap

818 permutations), and branch color represents the clade. Colored strips show the

819 source of isolation of each of the included genomes and the general category to

820 which the source belongs. Bar plots show the genome abundance enrichment in gut

821 metagenome samples compared to environmental samples calculated using

822 DESeq2; dots indicate taxa with significant enrichment in either host or

823 environmental biome (Adj. $P < 0.05$). The scale bar represents the number of amino

824 acid substitutions per site.

825

826 **Figure 2. *Methanomassiliicoccales* clades are widespread but not abundant**

827 **across a range of environments and animal hosts.** Combined abundance of

828 representative genomes of the EX (purple), FL (green), HA (orange) clades on

829 metagenome samples from diverse biomes: stomach (n = 12), foregut (23), large

830 intestine (66), fecal (44), desert (4), sand (12), grasslands (8), permafrost (22),

831 sediment (31), coastal (28), intertidal zone (25), lentic (6), groundwater (3), saline
832 (2), hypersaline (9) and Ice (10). Abundances calculated for individual genomes
833 using KrakenUniq and aggregated by clade. Y-axis in logarithmic scale, black points
834 indicate mean relative abundance in percentage, black bars indicate standard
835 deviation.

836

837 **Figure 3. Genome characteristics and adhesion protein repertoire of**
838 ***Methanomassiliicoccales* reflect division of the order into clades, although**
839 **members of the Clade FL not enriched in environmental biomes resemble**
840 **those of the Clade HA.** The phylogeny is the same as shown in Figure 1. The
841 colored strip summarizes the biome enrichment analysis. Heatmaps show genome
842 features including genome GC content (GC; range: 41.26 %, 62.74 %), genome
843 length (Len; 969.311 bp, 2.620.233 bp), and number of predicted genes (Genes;
844 1057, 2607) (blue scale); or repertoire of adhesion proteins: Sel1 containing proteins
845 (Sel1; 0, 29), Listeria-Bacteroides repeat containing proteins (List-Bact; 0, 26),
846 tetratricopeptide repeats (TPR; 7, 40), Ankyrin repeats (ANK; 0, 3), Leucine-rich
847 repeats (LRR; 0, 9), Fibronectin type III (FN3; 0, 20) domains, Bacterial Ig-like
848 domains (Ig-like; 0, 12), YadA-like domain (YadA; 0, 1) and adhesin-like proteins
849 (ALP; 0, 12) (gray scale; columns ordered by hierarchical clustering). On both
850 heatmaps the color intensity of each feature is relative to the maximum value of each
851 category. Scale bar represent the number of amino acid substitutions per site.

852

853 **Figure 4. Ordination of gene content of *Methanomassiliicoccales* group taxa by**

854 **phylogenetic clade rather than by biome enrichment.** Principal component

855 analysis of the gene cluster presence of taxa from clades FL (green), HA (orange)

856 and EX (purple). Highlighted points correspond to outliers: taxa either not

857 significantly enriched in environmental or gut biomes, or with enrichment opposite to

858 the expectation given their clade.

859

860 **Figure 5. Members of *Methanomassiliicoccales* are rare members of the human**

861 **gut microbiota.** Scatter plots of the genera A) *ca.* *Methanomethylophilus* and B)

862 *Methanomassiliicoccus* show that their prevalence and mean abundance is low

863 across most studies and populations (n = 4472; 35 datasets) with subjects from

864 Australia (AUT), China (CHN), Denmark (DNK), Ethiopia (ETH), Fijo (FJI), Great

865 Britain (GBR), Ghana (GHA), Israel (ISR), Madagascar (MDG), Mongolia (MNG),

866 The Netherlands (NDL), El Salvador (SLV), Sweden (SWE), Tanzania (TZA) and the

867 United States (USA).

868

869 **Figure 6. Coabundance networks of *Methanomassiliicoccus* (green node, dark**

870 **edges) and “*ca.* *Methanomethylophilus*” (orange node, light edges) in the**

871 **human gut largely overlap.** Both *Methanomassiliicoccales* genera are significantly

872 co-abundant (cyan edge). Their abundances are also coordinated with another

873 archaeon (blue node) and TMA-producing bacterial taxa (red nodes).

874

875 ***Table legends***

876 **Table 1.** InterPro, eggNOG and Prokka annotations of gene clusters significantly

877 enriched on clade HA compared to Clade FL. Four gene clusters with no annotation

878 were omitted.

879

880 ***Supplementary figure legends***

881 **Figure S1. *Methanomassiliicoccales* taxa from all clades are widespread but**

882 **not abundant across a range of environments and animal hosts.** The

883 abundance of members of the FL and HA clades is comparable within similar

884 biomes, in particular, animal derived metagenomes. Abundance of each

885 representative genome on diverse metagenome and environmental metagenome

886 samples colored by clade (FL: green, HA: orange, EX: purple). Abundances

887 calculated for individual genomes using KrakenUniq and aggregated by clade. Note

888 that the Y-axis is in logarithmic scale and each plot has a different scale. Black

889 points indicate mean relative abundance in percentage, black bars indicate standard

890 deviation. Metagenome samples from stomach (n=12), foregut (23), large intestine

891 (66), fecal (44), desert (4), sand (12), grasslands (8), permafrost (22), sediment (31),

892 coastal (28), intertidal zone (25), lentic (6), groundwater (3), saline (2), hypersaline

893 (9) and Ice (10).

894

895 **Figure S2. Small clusters of unknown function dominate the pangenome of the**

896 **order *Methanomassiliicoccales*.** Gene cluster frequency spectrum of the order

897 *Methanomassiliicoccales* separated by (A) unknown or (B) known function. (C)

898 Fraction of gene clusters belonging to each COG category per clade. Core clusters

899 were defined as present in $\geq 80\%$ of genomes of a clade; for the complete order,

900 gene clusters were present in $\geq 80\%$ of the included genomes and at least one

901 member of each clade. The proportion of clusters of unknown functions in the core

902 genome of each clade was large and varied between clades, ranging from 23.0 % in

903 Clade HA to 38.5 % in Clade EX. The proportion of unknown clusters was lowest in

904 the complete taxonomic order, where it only accounted for 14.7 % of gene clusters.

905 COG functional classification descriptions by groups. Information Storage and

906 processing: (B) Chromatin structure and dynamic, (J) Translation, ribosomal

907 structure and biogenesis, (K) Transcription, (L) Replication, recombination and

908 repair. Cellular processes and signaling: (D) Cell cycle control, cell division,

909 chromosome partitioning, (M) Cell wall/membrane/envelope biogenesis, (N) Cell

910 motility, (O) Post translational modification, protein turnover, chaperone, (T) Signal

911 transduction mechanisms, (U) Intracellular trafficking, secretion, and vesicular,

912 transport, (V) Defense mechanisms, (Z) Cytoskeleton. Metabolism: (C) Energy

913 production and conversion, (E) Amino acid transport and metabolism, (F) Nucleotide

914 transport and metabolism, (G) Carbohydrate transport and metabolism, (H)

915 Coenzyme transport and metabolism, (I) Lipid transport and metabolism, (P)
916 Inorganic ion transport and metabolism, (Q) Secondary metabolites biosynthesis,
917 transport and catabolism. Poorly characterized: (X) No annotation retrieved, (S)
918 Function unknown.

919

920 ***Supplementary table legends***

921 **Table S1.** CBI assembly accession, genome characteristics, study information and
922 source of isolation of 71 publicly available genomes from the order
923 Methanomassiliicoccales retrieved from NCBI in June 2018, plus the ca. *M. alvus*
924 MAG here reported. Study accession and title of UBA genomes obtained from
925 supplementary tables of Parks et al., 2017 (doi: 10.1038/s41564-017-0012-7),
926 otherwise, obtained from NCBI bioproject.

927

928 **Table S2.** SRA and MGnify accession information of publicly available metagenome
929 samples from gastrointestinal and environmental biomes

930

931 **Table S3.** SRA, study and country information of publicly available human gut
932 metagenome samples

933

934 **Table S4.** Prevalence and mean abundance of candidatus *Methanomethylophilus*
935 and *Methanomassiliicoccus* across multiple human populations.

936

937 **Table S5.** Intraclass correlation coefficients (ICC) of and FRD-adjusted P values of

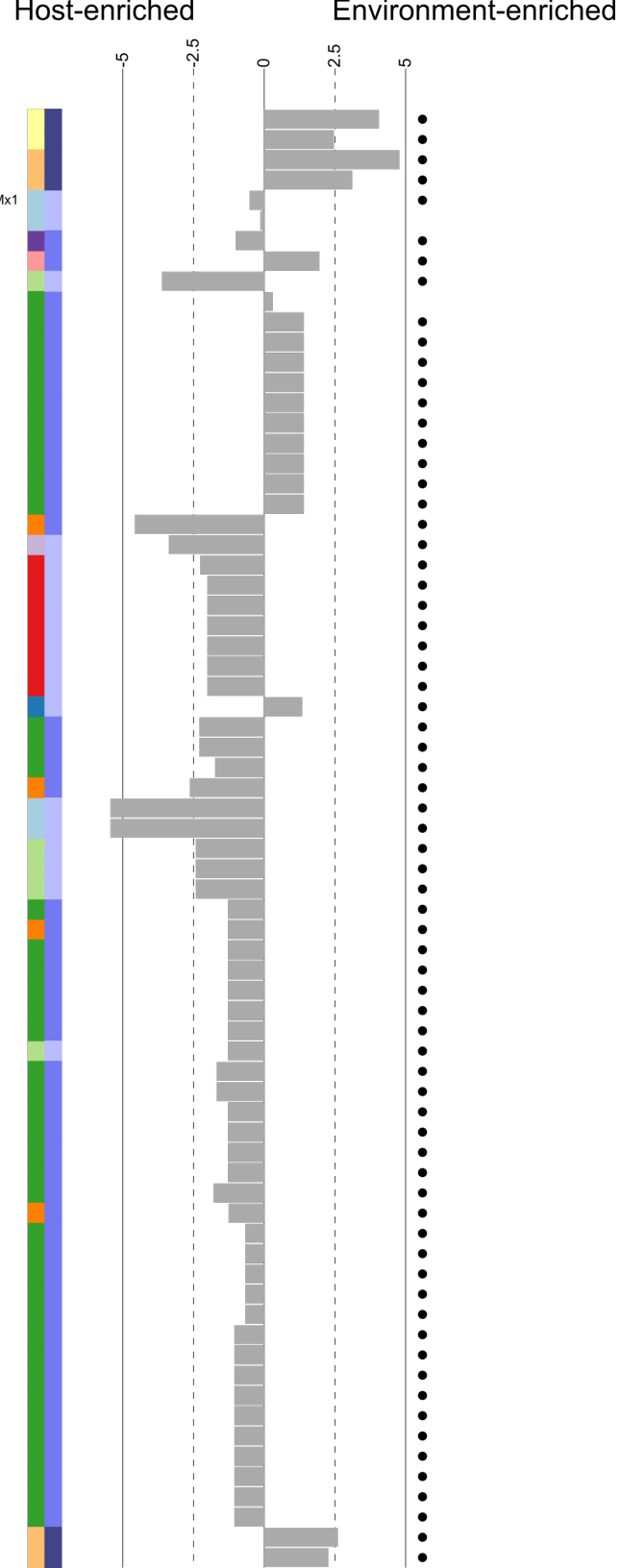
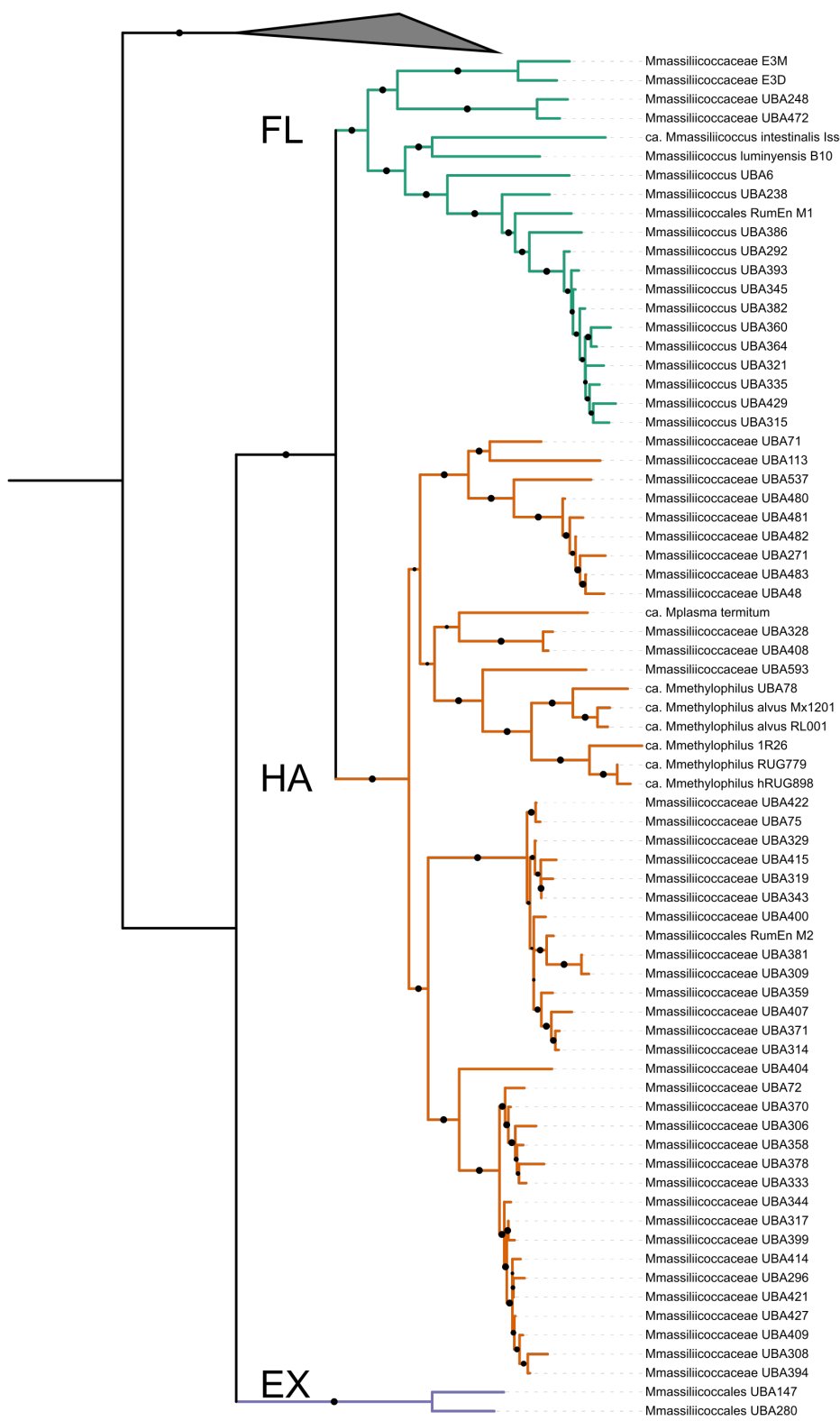
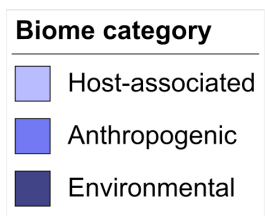
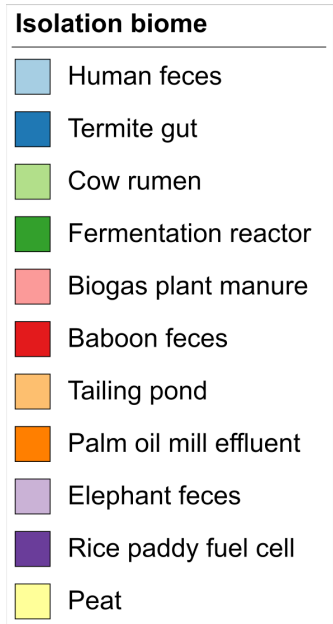
938 relative abundances *Methanomassiliicoccus* and other control taxa on monozygotic

939 and dizygotic twins

940

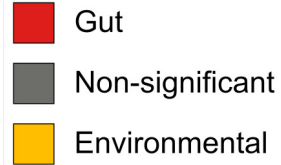
941

Tree scale: 0.1

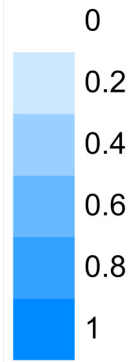


Tree scale: 0.1

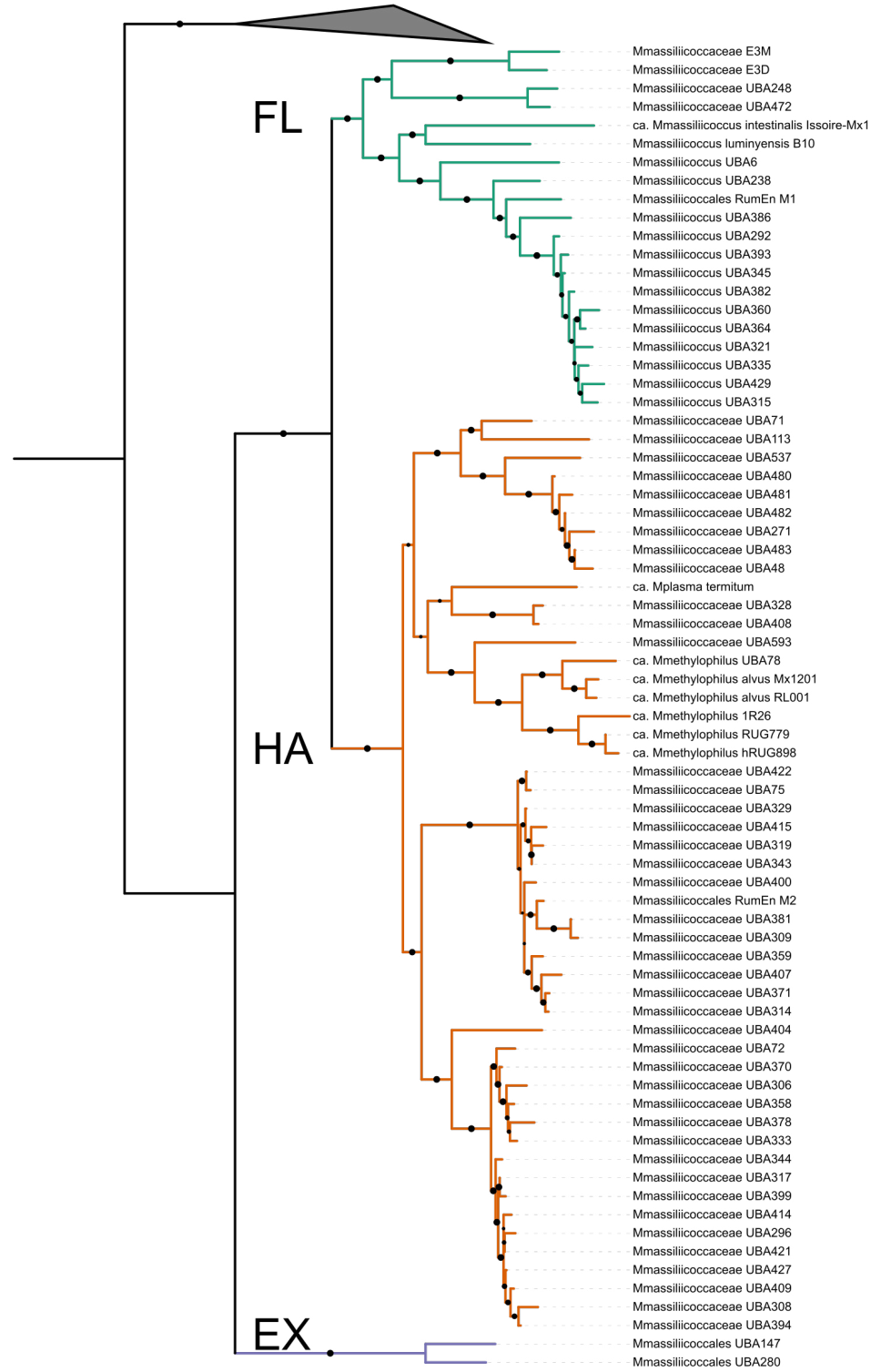
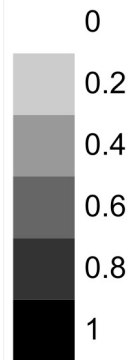
Biome Enrichment



Genome Characteristics

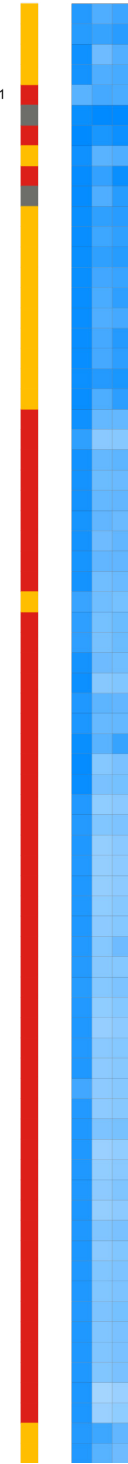


Adhesion proteins

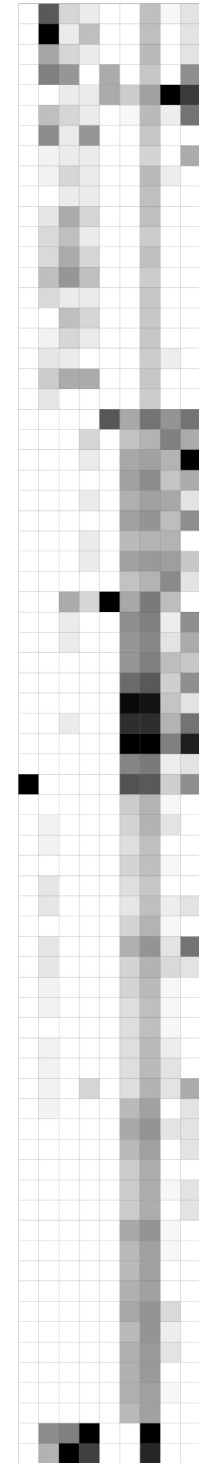


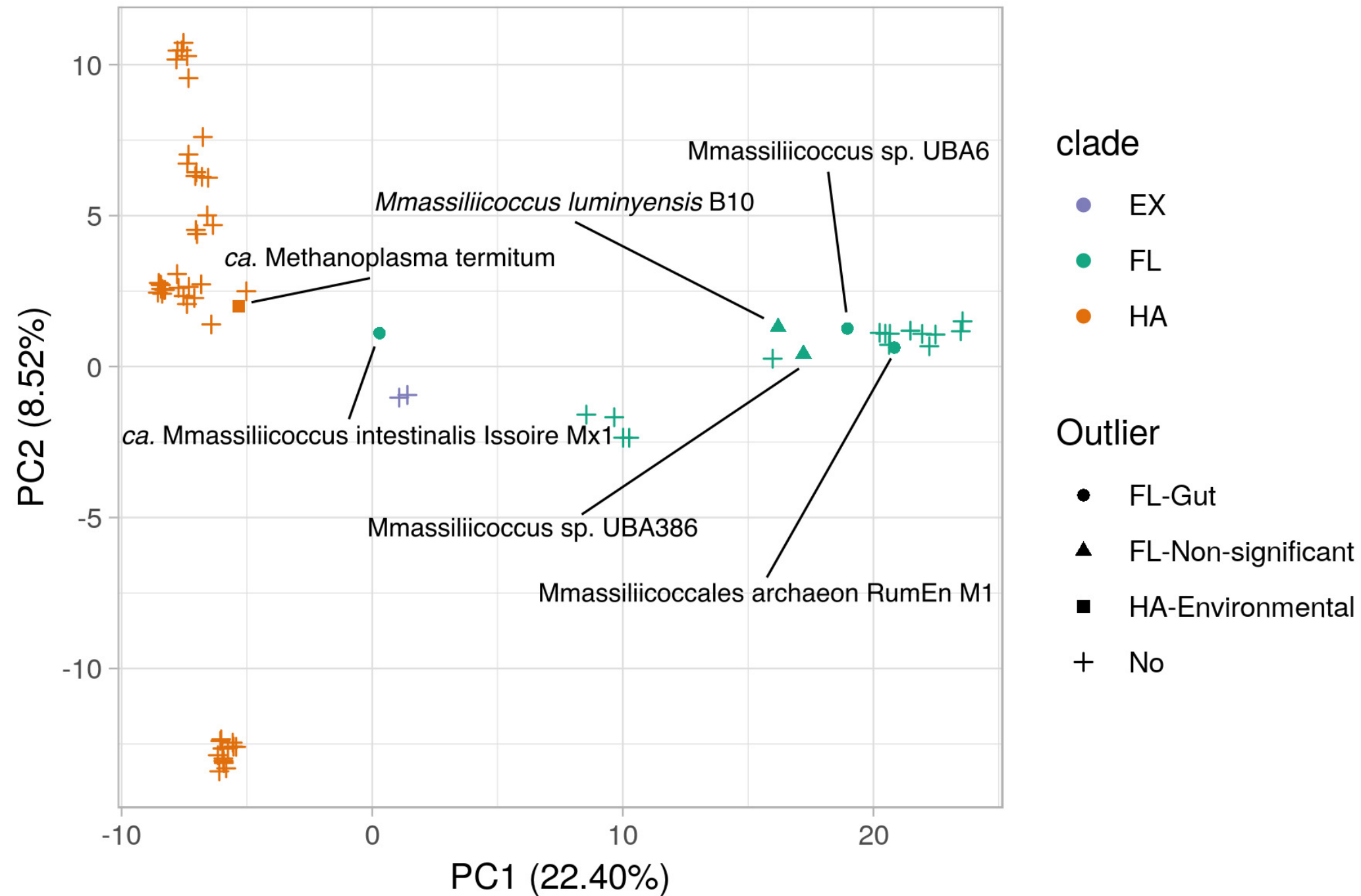
- Mmassiliococaceae E3M
- Mmassiliococaceae E3D
- Mmassiliococaceae UBA248
- Mmassiliococaceae UBA472
- ca. Mmassiliococcus intestinalis Issoire-Mx1
- Mmassiliococcus luminyensis B10
- Mmassiliococcus UBA6
- Mmassiliococcus UBA238
- Mmassiliococcales RumEn M1
- Mmassiliococcus UBA386
- Mmassiliococcus UBA292
- Mmassiliococcus UBA393
- Mmassiliococcus UBA345
- Mmassiliococcus UBA382
- Mmassiliococcus UBA360
- Mmassiliococcus UBA364
- Mmassiliococcus UBA321
- Mmassiliococcus UBA335
- Mmassiliococcus UBA429
- Mmassiliococcus UBA315
- Mmassiliococaceae UBA71
- Mmassiliococaceae UBA113
- Mmassiliococaceae UBA537
- Mmassiliococaceae UBA480
- Mmassiliococaceae UBA481
- Mmassiliococaceae UBA482
- Mmassiliococaceae UBA271
- Mmassiliococaceae UBA483
- Mmassiliococaceae UBA48
- ca. Mplasma termitum
- Mmassiliococaceae UBA328
- Mmassiliococaceae UBA408
- Mmassiliococaceae UBA593
- ca. Mmethylophilus UBA78
- ca. Mmethylophilus alvus Mx1201
- ca. Mmethylophilus alvus RL001
- ca. Mmethylophilus 1R26
- ca. Mmethylophilus RUG779
- ca. Mmethylophilus hRUG898
- Mmassiliococaceae UBA422
- Mmassiliococaceae UBA75
- Mmassiliococaceae UBA329
- Mmassiliococaceae UBA415
- Mmassiliococaceae UBA319
- Mmassiliococaceae UBA343
- Mmassiliococaceae UBA400
- Mmassiliococcales RumEn M2
- Mmassiliococaceae UBA381
- Mmassiliococaceae UBA309
- Mmassiliococaceae UBA359
- Mmassiliococaceae UBA407
- Mmassiliococaceae UBA371
- Mmassiliococaceae UBA314
- Mmassiliococaceae UBA404
- Mmassiliococaceae UBA72
- Mmassiliococaceae UBA370
- Mmassiliococaceae UBA306
- Mmassiliococaceae UBA358
- Mmassiliococaceae UBA378
- Mmassiliococaceae UBA333
- Mmassiliococaceae UBA344
- Mmassiliococaceae UBA317
- Mmassiliococaceae UBA399
- Mmassiliococaceae UBA414
- Mmassiliococaceae UBA296
- Mmassiliococaceae UBA421
- Mmassiliococaceae UBA427
- Mmassiliococaceae UBA409
- Mmassiliococaceae UBA308
- Mmassiliococaceae UBA394
- Mmassiliococcales UBA147
- Mmassiliococcales UBA280

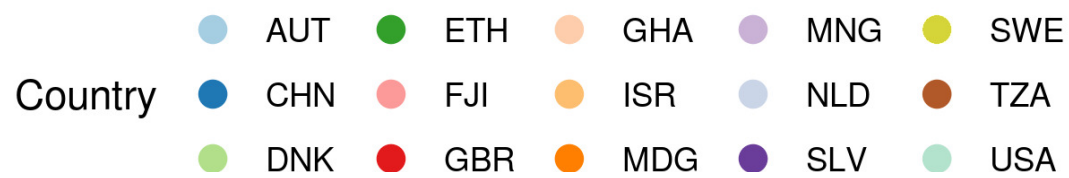
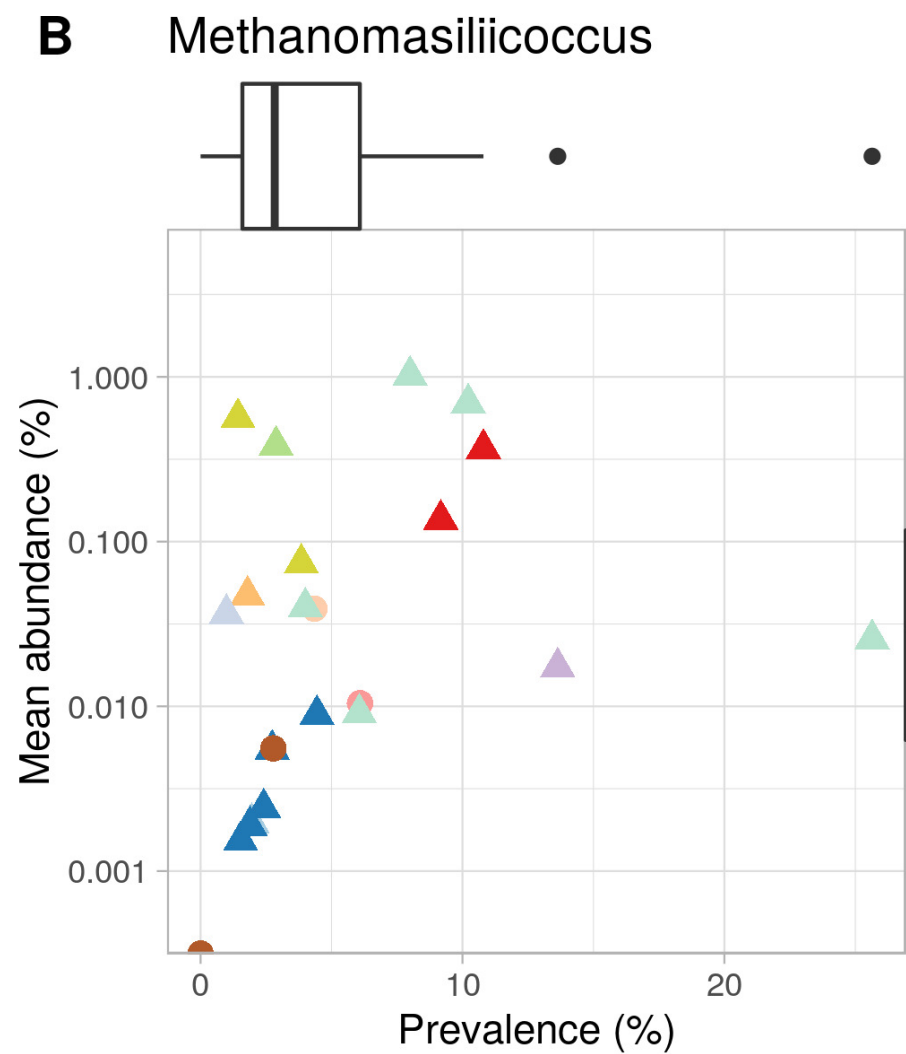
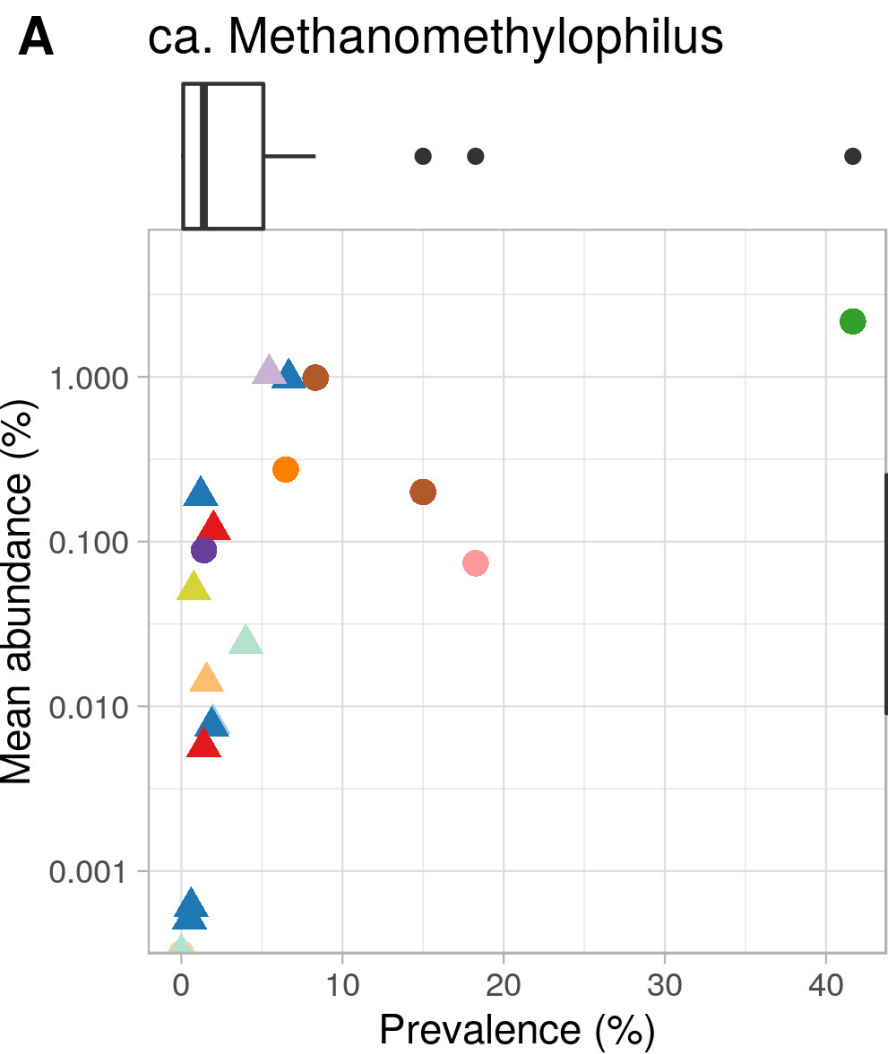
GC
Len
Genes

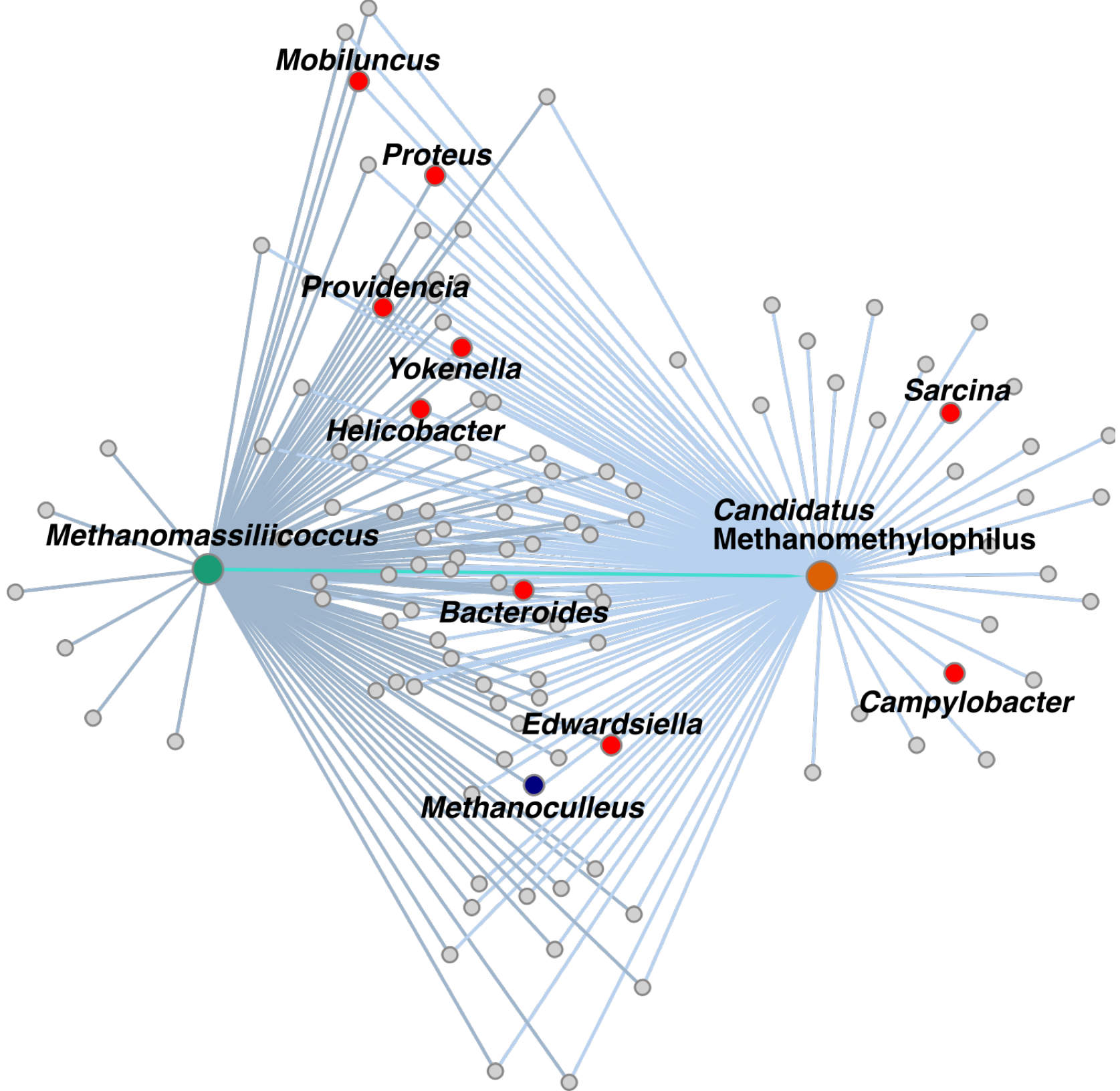


YadA
FN3
ALP
Ig_like
ANK
Sel1
TPR
List_Bact
LRR









Interpro accession	Interpro annotation	NOG accession	COG category	Prokka gene name	Prokka annotation
IPR001086	Prephenate dehydratase	COG0077@NOG	E	pheA	Prephenate dehydratase
IPR002657	Bile acid:sodium symporter/arsenical resistance protein Acr3	COG0385@NOG	S	-	hypothetical protein
IPR002701	Chorismate mutase II, prokaryotic-type	COG1605@NOG	E	aroQ	Chorismate mutase
IPR002732	Holliday junction resolvase Hjc	COG1591@NOG	L	rutD	Putative aminoacrylate hydrolase RutD
IPR003761	Exonuclease VII, small subunit	COG1722@NOG	L	xseB	Exodeoxyribonuclease 7 small subunit
IPR006357	HAD-superfamily hydrolase, subfamily IIA	COG0647@NOG	G	gph	Glyceraldehyde 3-phosphate phosphatase
IPR013022	Xylose isomerase-like, TIM barrel domain	11IHC@NOG	L	-	hypothetical protein
IPR015867	Nitrogen regulatory protein PII/ATP phosphoribosyltransferase, C-terminal	COG3323@NOG	S	-	hypothetical protein
IPR019271	Protein of unknown function DUF2284, metal-binding	11RTN@NOG	S	-	hypothetical protein
IPR029068	Glyoxalase/Bleomycin resistance protein/Dihydroxybiphenyl dioxygenase	-	X	-	hypothetical protein